c-VACNT™ enabled Fluid Reactor Innovations

K Strobl*, S. Gainey *, Ajay Kumar* and Ajay Kumar*

*CVD Equipment Corporation, 355 S. Technology Drive, Central Islip, NY 11722

ABSTRACT

We have developed a novel, patent-pending, fluid reactor system that is targeted for (1) improved Extracorporeal Membrane Oxygenation (ECMO) devices utilized in heart-lung machines by enabling i) their use for an extended duration ii) manufacture of ECMO devices that operate on air instead of pure oxygen for special logistically challenged situations, iii) reduce the amount of donor blood needed for an operation and iv) reduce the pressure needed for operation and (2) provide enhancements for other fluid reaction based applications such as dialysis, chemical, pharma and biomaterial manufacturing; filtration; fluid gasification and degasification; desalination; etc. These fluid reactor devices are enabled by a family of novel Reactor Core Elements (RCE) made from a free-standing, self-supporting, carbon-infiltrated c-VACNT™ material.

Keywords: Fluid Reactor, ECMO, carbon infiltration, VACNT, c-VACNT™

1 C-VACNT™ DEVELOPMENT

We have developed a wide range of free-standing carbon infiltrated vertically aligned CNT (VACNT) material structures optimized for maximizing the performance of a given product. Our development incorporates a range of proprietary manufacturing processes and equipment solutions to produce c-VACNT™ for our customers' proprietary product development needs.

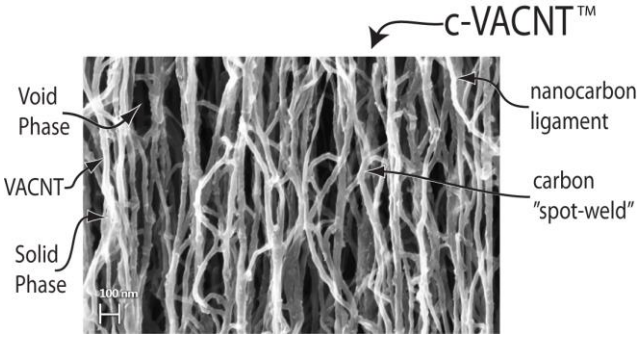

Figure 1: c-VACNT™ material nano structure

The c-VACNT™ material is an all nano-carbon based open-pore cellular network having a tortuous bi-continuous phase structure. The material is comprised of a tunable void phase and a solid phase structure made of "spot-welded" ligaments having a tunable strength and stiffness. Patterned VACNTs array structures are first grown on a photolithographically processed catalyst wafer and then overcoated with a carbon film having a tunable average film thickness, *T*, resulting in local "spot-welding" of individual carbon nanotubes (CNTs) that are separated by a distance, D < 2T, as indicated in Fig. 1 and 2.

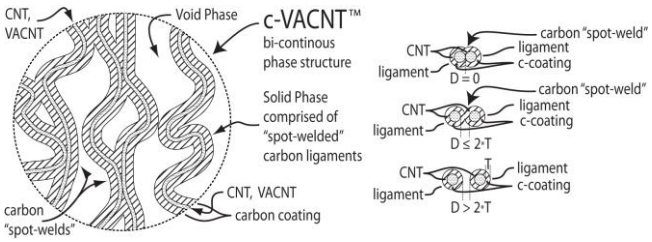

Figure 2: c-VACNT™ carbon "spot-welding" process

Both the VACNT growth and the carbon infiltration process have been implemented on a First Nano® EasyTube® 3000 system (Fig. 3) resulting in processing capacity of > 90 – 100mm wafers/week.

Figure 3: c-VACNT™ processing CVD system

After the c-VACNT™ growth process, the resulting c-VACNT™ structures are separated from their growth wafers and further processed in an application specific manner.

Our c-VACNT™ production capability enables the manufacturing of a wide variety of c-VACNT™ structures with the change of the photolithographic mask and CVD process tuning.

2 C-VACNT™- RCE

Fig. 4 shows a range of free-standing c-VACNT™ structures in the form of proprietary RCEs [1] with each c-VACNT™ structure tuned for both porosity and strength.

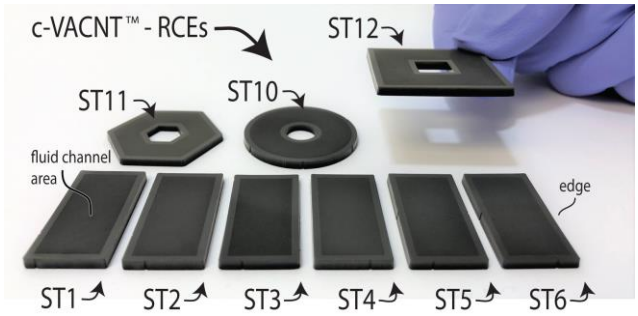

Figure 4: A range of c-VACNT™ - RCE types (Table2)

These c-VACNT™ - RCEs have a fluid channel area that is shown in Fig. 4 as being surrounded by an edge zone with the thickness, ε. Fig. 5 shows a magnified SEM image of a top and cross-sectional view of the fluid channel area of a cleaved ST12 type sample. This area contains cylindrical perforations (channels) spaced in a periodic hexagonal pattern with a non-tortuous flow path oriented parallel to the VACNT growth direction extending from the top to the bottom of the respective c-VACNT™ structure. The open pore c-VACNT™ material structure (Fig. 1) that surrounds these channels effectively forms a sidewall with asymmetric slit pores (typically *20-100 nm x 200-1,000 nm*). This c-VACNT™ structure thus forms a membrane-like fluid channel side wall, having a surface area $SA_{FC} = \pi * d * h$, with *d* representing the diameter of the channel and *h* its height.

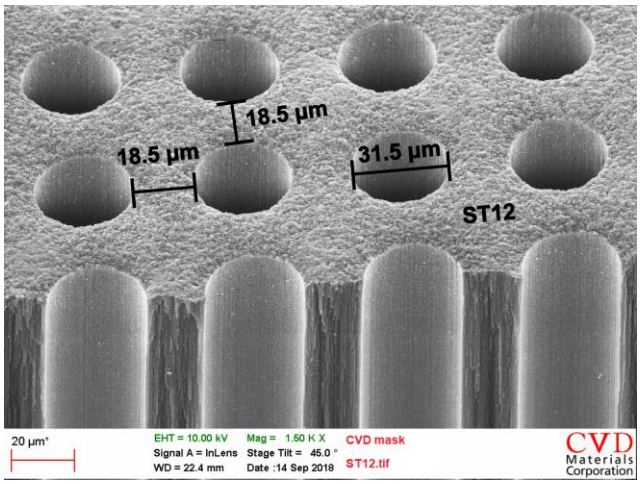

Figure 5: c-VACNT™-RCE with a non-tortuous flow path

This membrane-like sidewall separates the space filled with c-VACNT™ material from the space inside the through-channels and thus provides a selective transmission function that can be utilized for fluid processing applications.

Additional surface coating(s) of the solid phase c-VACNT™ material fluid channel sidewalls and/or their neighboorhood can further optimize this selective transmission function and/or overall performance of such c-VACNT™ - RCEs for selected fluid processing applications. For example, a hydrophobic coating helps to minimize and/or delay water penetration into the bulk structure (void space) for water-based liquids (i.e., blood).

3 HOLLOW FIBER - C-VACNT™- RCE

Many types of fluid reactors having a primary and secondary fluid channel with respective inflow and outflow ports incorporate over 10,000 parallel connected, polymer-based (i.e., polypropylene) RCEs in the form of individual porous Hollow Fibers (HF). These HFs have a sidewall with symmetric or asymmetric slit pores (typically aligned with the HF axis) with width, *w*, and length, *l*, an overall sidewall volume porosity, ρ, and an outer Surface Area, SA. The inner lumen diameter, ϕ, and sidewall thickness, *t*, of these HFs, are typically limited by i) commercially available HF product selections and ii) by commercially viable manufacturing yield requirements. Creating a localized fluid tight seal at the end of each HF bundle with minimal sidewall integrity damage is needed to prevent cross-leakage between the primary and secondary fluid path. The active porous wall membrane surface or an additional thin film membrane supported by it separates the two fluids. Thus all inside and outside sidewalls of each HF are in contact with only either a primary or secondary fluid. The total active membrane surface area provides a controlled and selective cross-talk between the fluids.

HF vendor model	ϕ [µm]	t [µm]	w/l [µm]	ρ [%]	Ψ [%]	S/V [m²/m³]
Company 1	*244*	*28*	*0.03 0.2*	*40*	*50*	*6,667*
Company 2	*200*	*22*	*0.04*	*40-55*	*50*	*8,163*
Company 3	*280*	*50*	*0.2*	*NA*	*50*	*5,263*

Table 1: Hollow Fiber key parameters and S/V values

HFs reactor cores have a packing density, Ψ, resulting in an active membrane surface area to reactor core volume ratio, S/V. Table 1 lists key parameters and S/V values for HF based reactor cores for some commercially available HFs.

Table 2 lists key parameters for the c-VACNT™ - RCE types ST1-ST12 shown in Fig. 4 for a chosen height $h = 2$ *mm* and edge width $\varepsilon = 1.5$*mm*. *N* represents the number of fluid channels, *g* represents the minimal distance between two neighboring channels and SA the total active membrane

surface area. To build higher capacity, RCs multiple c-VACNT™ - RCEs can be parallelly and/or serially connected in a sealed manner to form a respective RC [1]. To show the potential for this new RC/RCE capability for novel fluid reactor types and applications, Table 2 lists other possible c-VACNT™ - RCE types that have been shown to be commercially volume manufacturable with the thus far developed processing capabilities $\phi \geq 5\ \mu m$, $g \geq 5\ \mu m$, $h \leq 5mm$, $\varepsilon \geq 0\ mm$ of the c-VACNT™ discussed above.

Type	ϕ [µm]	g [µm]	*N*	*SA* [cm²]	ρ [%]	*S/V* [m²/m³]
ST1	*46.5*	*18.5*	*89K*	*260*	*34*	***28,900***
ST2	*36.5*	*18.5*	*124K*	*284*	*29*	***31,529***
ST3	*26.5*	*18.5*	*185K*	*308*	*23*	***34,246***
ST4	*21.5*	*18.5*	*235K*	*317*	*19*	***35,209***
ST5	*16.5*	*18.5*	*304K*	*317*	*15*	***35,215***
ST6	*11.5*	*18.5*	*416K*	*309*	*10*	***33,420***
ST10	*41.5*	*18.5*	*153K*	*399*	*29*	***28,250***
ST11	*31.5*	*28.5*	*195K*	*386*	*26*	***33,014***
ST12	*31.5*	*18.5*	*281K*	*556*	*24*	***30,878***
ST20	*10.0*	*10.0*	*936K*	*588*	*16*	***65,362***
ST21	*5.0*	*5.0*	*3,7M*	*1,176*	*16*	***131K***

Table 2: c-VACNT™-RCE key parameters and S/V values

The S/V values for the c-VACNT™ - RCEs described in Table 2 can be >10X larger than those for HFs based RCs. c-VACNT™ - RCEs, therefore, become key components for designing and building higher performance fluid reactors for at least selected performance challenged applications.

4 FLUID REACTOR PERFORMANCE

A fluid reactor is used to compositionally modify an input fluid to create a respective output fluid with the aid of a secondary fluid. Typically there is a primary fluid path and a secondary fluid path with a respective input and output port (4 port device) which is separated by a membrane that has different transmission properties for different fluid components. Many fluid reactor applications [2] have been developed since HFs became commercially available as RCEs for building RCs. The hollow fiber membranes market size will exceed USD 6B by 2025; according to a research report by Global Market Insights, Inc. Applications of HF range from filtration, chemical recovery, fine chemical processing, pharmaceuticals, biotechnology, medicine ECMO and dialysis, wastewater treatment, desalination, and others with each market having a unique set of functional requirements to make them commercially viable.

To better understand how these novel c-VACNT™ RCEs might provide an advantage over HFs for fluid reactor applications, a few key parameter relationships need to be understood. The fluid pressure drop ΔP across a bundle N fluid channels arranged in a periodic hexagonal pattern over a Cross-sectional Area, CA, having a diameter, ϕ, gap, g, and length, h, through which a fluid with a viscosity, η, is flowing at a flow rate, F, can be derived from Poiseuille's equation.

$$\Delta P = \frac{F * 128 * \eta * h}{N * \pi * \phi^4} \approx \frac{F * \sqrt{3} * 64 * (\phi + g)^2 * \eta * h}{CA * \pi * \phi^4} \quad for\ N >> 1 \quad (1)$$

Equation (1) shows that the pressure drop, ΔP, is proportional to length, h, and inversely proportional to diameter, ϕ. Equation (2) shows the dependence of the ratio S/V of the surface area per RCE volume on diameter, ϕ, and gap, g.

$$S/V = \frac{N * \pi * \phi * h}{CA * h} \approx \frac{2 * \pi * \phi}{\sqrt{3} * (\phi + g)^2} \quad for\ N >> 1 \quad (2)$$

For a given g the value of S/V is maximized when $\phi = g$. Entering this condition into equation (1) and (2) results in equation (3).

$$\Delta P \approx \frac{F * \sqrt{3} * 256 * \eta * h}{CA * \pi * \phi^2},\ S/V \approx \frac{\pi}{\sqrt{12} * \phi} \quad for\ N >> 1,\ \phi = g \quad (3)$$

Since the c-VACNT™ structure can be manufactured with fluid channels down to $\phi \geq 5\ \mu m$, $g \geq 5\ \mu m$ much higher S/V values can be achieved (compare Table 1 and 2).

The flow velocity profile inside a round fluid channel follows the parabolic Poiseuille flow distribution having a maximum flow velocity v_{max} at its center that can be calculated from the various RCE parameters as shown below.

$$v_{max} = \frac{8 * F}{N * \pi * \phi^2} \approx \frac{\sqrt{48} * F}{\pi * CA} * \frac{(\phi + g)^2}{\phi^2} \quad for\ N >> 1 \quad (4)$$

For a saturable fluid reaction process (i.e. water or blood oxygenation) where a secondary fluid component (i.e. O_2) gets absorbed into all the available quantity of a primary fluid (i.e. water or blood) until approximately a maximum quantity of output fluid (i.e. $\approx 100\%$ dissolved O_2 concentration) has been produced, a critical diffusion reaction time, t_c, is defined as the average diffusion time it takes for such a fluid component to diffuse from the cylindrical-shaped side wall to its centerline. Equation (5) relates the critical diffusion reaction time, t_c, to the critical height h_c of a fluid channel above which (with sufficient available secondary fluid quantity at the channel sidewall) even the fastest moving portion of the incoming primary fluid has already been fully converted into a respective primary output fluid, i.e. above which the production rate of the respective fluid reactor saturates.

$$h_c = v_{max} * t_c \quad (5)$$

The critical diffusion reaction time, t_c, dependence on the channel diameter, ϕ, and diffusion constant, D, can be derived from a diffusion solution C(t, r) of the Fick's second diffusion law[3] for the case of an axially symmetric

diffusion in an infinitely long cylinder with diameter, ϕ, and with the following boundary conditions: (i) the primary fluid entering a fluid channel has a uniform starting saturation concentration C_0, i.e. $C(0, r) = C_0$; (ii) the diffusion substance penetrates the fluid channel sidewall and diffuses towards the center of the channel; (iii) when the diffusing substance contacts the primary fluid across the sidewall, the boundary layer is instantly fully saturated and remains independent of the primary fluid flow rate, i.e. $C(t, r = \phi/2) = C_\infty$ with C_∞ representing the fully saturated primary fluid concentration; and (iv) the diffusion solution $C(t, r = \phi/2 - x)$ for $x << \phi/2$ is very similar to the diffusion solution for a semi-infinite domain. Solving for the time, t_c, when the diffusion front just reaches the center line $r = 0$ yields equation (6).

$$t_c \approx \frac{\phi^2}{16 * D * \upsilon_c^2} \qquad with \ \ \upsilon_c \approx 3.599703 \qquad (6)$$

Equation (6) connects the critical reaction time, t_c, to the channel diameter, ϕ, and diffusion constant, D. υ_c is a constant related to the geometrical difference between a one-dimensional and a radially symmetric diffusion case.

The theoretically maximum primary fluid flow rate F_{max} and corresponding pressure drop, ΔP_{Fmax}, for an RCE with height, h, for which a fully saturated output fluid can still be produced, i.e., $h = h_c$, can be derived from the equation (7) and (8).

$$F_{max}(h = h_c) = 2 * h * N * \pi * D * \upsilon_c^2 \approx \frac{4 * h * \pi * D * \upsilon_c^2 * CA}{\sqrt{3} * (\phi + g)^2} \qquad (7)$$

$$\Delta P_{Fmax}(h = h_c) = \frac{128 * h * \eta * F_{max}}{\pi * \phi^4 * N} = \frac{256 * \eta * D * \upsilon_c^2 * h^2}{\phi^4} \qquad (8)$$

The combination of higher membrane surface area volume packing density, the ability to create robust c-VACNT™ - RCEs with channels having a smaller diameter, and/or a tighter packing density (smaller g) and a short and straight (non-tortuous) flow path leads to design opportunities for novel fluid reactors. Fluid reactors that have one or more key performance enhancements (i.e., smaller processing volume, a smaller pressure drop, ΔP, a faster reaction time, less tortuous primary fluid path, etc.) will enable advancing the state of the art in performance challenged fluid reactor applications.

5 POTENTIAL APPLICATIONS

One potential application of these c-VACNT™ - RCEs and related assembled RCs are potentially higher efficiency fluid reactor systems targeted to improve existing ECMO devices utilized in heart-lung machines during cardiopulmonary bypass or cardioplegia surgery. Possible improvement opportunities of existing ECMO devices are smaller priming volume (taking advantage of the higher S/V value), a less tortuous blood flow path (see in Fig. 5 the non-tortuous blood flow path inside the straight and short (mm tall) fluid channels) and a smaller pressure drop, ΔP, cross the RC.

These improvements should help minimize complications of related surgeries, thereby improving the quality of care and potentially be a reason for the medical industry to switch from HF based ECMOs to this ECMOs based on c-VACNT™ - RCEs. If it can be shown that these c-VACNT™ based ECMO devices can be made sufficiently bio-compatible (by applying biocompatible coatings as are already commercially available) and are safer to use or at a minimum need less priming volume, they could enable the design and building of next-generation ECMOs for extended blood oxygenation needs.

If the priming volume of an ECMO device can be made ≈ 5X smaller than that of the HF technology for the same blood flow capacity (adult male, for example) without increasing the pressure drop ΔP across the ECMO device, this potentially enables the manufacture of ECMO devices that operate on air instead of pure oxygen useful in special logistically challenging situations[4]. It would also potentially enable the manufacture of portable "artificial" lungs.

Given the large design parameter space and the inherent chemical stability of the c-VACNT™ material, we anticipate that other pharmacological, biological and other high-value chemical processing opportunities will emerge that can piggyback on the development and scale-up efforts that are ongoing for the initially identified advanced ECMO device development opportunities.

6 SUMMARY

We have shown the manufacturability of novel free-standing c-VACNT™ structures from an all nano-carbon based open-pore cellular network having a tortuous bi-continuous phase structure that is comprised of carbon "spot-welded" VACNTs ligaments and void space. We showed how to manufacture a novel fluid reactor core element in the form of a c-VACNT™ - RCE containing a high density array of fluid channels having a diameter $\phi \geq 5\ \mu m$, a minimal channel gap $g \geq 5\ \mu m$, a height $h \leq 5$ mm and an edge exclusion zone width $\varepsilon \geq 0\ mm$. We have shown how these novel RCE structures can be analyzed for identifying novel performance opportunities that could lead to next-generation fluid reactors in performance challenged applications. Potential benefits of these c-VACNT RCE's for advancing the state of the art artificial lung applications (ECMO) have been shown.

REFERENCES

[1] US Pat. Application 62754375, Fluid Reactors

[2] Handbook of Industrial Membranes, K. Schott Elsevier Advanced Technology

[3] Cho-Laing Tsai, Ching-Chang Lin, 23 Journal of Marine Science and Technology 133-141 (2015)

[4] K.S., S.G., A.K, A.K., Air Powered Artificial Lungs and other High Efficiency Fluid Reactors Innovations, Techconnect 2019